

Melt and glass structure in the $\text{Al}_2\text{O}_3\text{--CaO--LaPO}_4$ system studied by ^{27}Al and ^{31}P NMR, and by Raman scattering

S. Boucher^a, J. Piwowarczyk^b, R.F. Marzke^{b,*}, B. Takulapalli^c,
G.H. Wolf^a, P.F. McMillan^d, W.T. Petuskey^a

^a Department of Chemistry and Biochemistry, Arizona State University, Tempe, AZ 85287-1604, USA

^b Department of Physics and Astronomy, Arizona State University, Tempe, AZ 85287-1504, USA

^c Science and Engineering Materials Program, Arizona State University, Tempe, AZ 85287-1704, USA

^d Royal Institution of Great Britain, Davy-Faraday Research Laboratory, 21 Albemarle St., London W1S 4BS, UK

Abstract

NMR chemical shift and Raman scattering measurements have been performed on molten and drop-quenched samples of the La-monazite containing ternary system $\text{Al}_2\text{O}_3\text{--CaO--LaPO}_4$. In $\text{Al}_2\text{O}_3\text{--LaPO}_4$ melts without CaO modifier, the observed chemical shift of ^{27}Al increases linearly towards ~ 72 ppm with increasing LaPO_4 . For C_{12}A_7 ($\text{Ca}_{12}\text{Al}_{14}\text{O}_{33}$) melts, increasing LaPO_4 leads initially to little change in the strongly tetrahedral ^{27}Al chemical shift (~ 85 ppm), but between 25 and 50% LaPO_4 the shift sharply decreases, indicating strong Al bonding changes. Liquid Ca_xLaPO_4 samples exhibit only moderate shift variations with LaPO_4 content. These dependences of ^{27}Al chemical shifts upon melt composition are reflected in substantial observed differences between molten and quenched samples, and may be related to the strong variations seen in physical properties of higher phosphate glasses. Quenched samples along the $\text{Al}_2\text{O}_3\text{--LaPO}_4$ join fractionate into distinct phases, but CaO content acts to suppress phase separation and often results in glass formation. Raman, ^{27}Al and ^{31}P NMR spectra of glassy samples indicate a structure based upon orthophosphate groups, each associated with one or more Al atoms in P–O–Al linkages. At 75% monazite content X-ray spectra of quenched samples show the presence of the crystalline double phosphate $\text{LaCa}_3(\text{PO}_4)_3$.
© 2005 Elsevier Ltd. All rights reserved.

Keywords: Spectroscopy; Al_2O_3 ; Glass ceramics; Refractories; NMR

1. Introduction

The refractory compound La-monazite (LaPO_4) has recently attracted interest because of its potential usefulness in extreme environments, in applications such as coatings for aircraft engine turbines or heat-resistant tiling for space vehicles. Industrial processing involves the interaction of monazite with ceramics, and to broaden understanding of this subject we have undertaken the study of a ceramic multi-component system containing La-monazite as a major constituent.

Samples belonging to the system $\text{Al}_2\text{O}_3\text{--CaO--LaPO}_4$, with monazite concentrations from 2 to 100 mol%, were ex-

amined by ultra high-temperature ^{27}Al NMR in the molten state^{1–4} and by conventional NMR of aluminum and phosphorus at room temperature. NMR allows monitoring of the Al and P chemical environments via shifts in the NMR frequencies of the nuclei studied, as explained below. The separate ranges of ^{27}Al chemical shifts for four-, five-, and six-fold oxygen coordination, as well as the ranges of ^{31}P shifts for different PO_4 tetrahedral unit linkages, are strong indicators of Al–O and P–O bonding. Drop-quenched samples were monitored for composition, uniformity and crystallinity via electron microprobe measurements and X-ray diffraction. Most of the samples containing CaO were found to be glassy, whereas CaO-free quenched samples separated into their Al_2O_3 and LaPO_4 constituent phases. Raman spectra of the glassy samples show vibrational modes found in widely studied phosphate glasses, which involve structures

* Corresponding author.

E-mail address: Robert.Marzke@asu.edu (R.F. Marzke).

with groups of atoms that move together or in opposition. The presence of these modes in the spectra reveals the presence of such groups, e.g., PO₄ tetrahedra, and is thus highly diagnostic of the nanostructure of the glass.

2. Experimental

Ultra high-temperature measurements of the chemical shift of ²⁷Al were performed between 2000 and 2500 °C on molten samples levitated in the bore of a superconducting magnet via an Ar gas flow through a convergent–divergent nozzle machined from BN. NMR spectra were taken on a Varian CMX Infinity 300 MHz solids instrument, equipped with a custom-built NMR probe. A CO₂ laser, square-wave modulated with variable pulse length to control output power, was employed for sample heating, and was operational throughout NMR data acquisition. Details are discussed elsewhere.^{1–5} While levitating, the molten sample is highly spherical, with diameter approximately 3 mm.

NMR is well known to be a powerful technique for the investigation of nanostructure, and it is worth reviewing the general approach used in acquiring NMR spectra. First, a sample is placed in a large dc magnetic field H_0 and subjected to a short, high-power pulse of electromagnetic radiation, whose radio frequency magnetic field H_1 is oriented along an axis perpendicular to H_0 . The angular frequency of this pulse is close to the natural angular frequency of precession ω_L of the individual nuclear magnetic moments of a sample about H_0 , called the Larmor frequency. This frequency is directly proportional to the dc field and the constant of proportionality, called the gyromagnetic ratio and denoted by γ , is characteristic of the particular nucleus under study, e.g., the proton (¹H) or aluminum (²⁷Al) nucleus.

The effect of the r.f. pulse is to rotate the sample's entire assembly of nuclear magnetic moments, i.e., its nuclear magnetization, about the axis of H_1 . Applying the pulse for a few microseconds, typically, results in rotation of the sample's initial magnetization by 90°, causing the magnetization to precess thereafter at the Larmor frequency ω_L in a plane perpendicular to H_0 (Fig. 1)

Second, the precessing magnetization induces oscillatory signals in a radio frequency coil surrounding the sample, which are amplified, recorded and then processed. The signals eventually decay, as the nuclear spins relax back to thermal equilibrium. The induced signal is thus called the free induction decay (FID), and in liquids or samples whose internal constituents are in rapid motion, it is usually a set of decaying exponentials.

Fourier transformation of the FID yields the NMR spectrum, which reflects the fact that nuclei in inequivalent positions in molecules or nanostructural units of a sample generally precess at measurably different frequencies. That is, the ratio ω_L/H_0 is usually not precisely the same for nuclei of the same isotope in structurally inequivalent

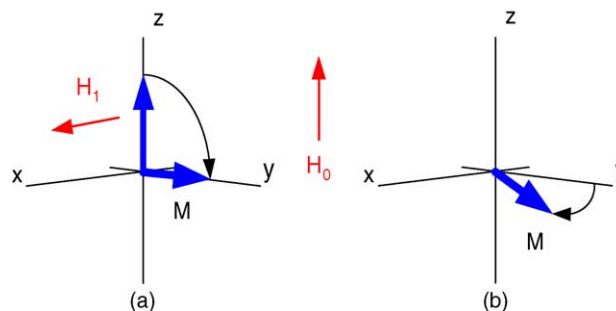


Fig. 1. (a) Application of a 90° r.f. pulse along the x-axis, rotating the nuclear magnetization about H_1 . (b) Larmor precession of the magnetization about the z-axis.

positions, in molecules or solids. These small differences are caused by well-known electronic interactions with the external dc field H_0 , and are known as chemical shifts. On the other hand, nuclei in chemically or physically identical positions in a sample have the same value of shift. The spectrum thus consists of lines at different frequencies for an isotope having different positions or chemical bonding within the sample, as can be seen in proton or ¹³C spectra of many organic compounds, as well as in ²⁷Al spectra of solid oxides. The intensity of each line is proportional to the number of nuclei in a given chemical environment, e.g., to the numbers of ²⁷Al nuclei in four-, five- or six-fold coordination with O. This yields valuable information about samples, especially those having no long-range or crystalline order.

In our measurements of chemical shifts, all observed frequencies were referenced to standards, such as Al³⁺ in ~1 M solutions of Al(NO₃)₃. Referencing in this manner is necessary because the shifts themselves are relatively small, of order parts per million (ppm). The dc field H_0 must also, therefore, be highly homogeneous over the sample.

In solid samples with fixed nuclei, precession frequencies even vary from one chemically equivalent position to another, owing to the presence of small random, internal magnetic fields. A common type of local field is the nuclear magnetic dipole field, which has for its source the nuclear moments of the sample itself and may produce NMR line widths of several kilohertz. In most liquid samples, however, extremely rapid movements of an atom or molecule cause a nucleus to sample many spin environments at rates far above the external field's contribution γH_0 to the precession frequency. The nucleus then precesses at a rate that is the motional average of the local field contributions to the frequencies of precession in a solid. For nuclear dipole fields this average is exactly zero. ²⁷Al spectra of a molten Al oxide sample thus exhibit a well-defined, single NMR frequency, with a shift that represents a weighted average of shifts for four-, five- and six-fold oxygen coordination, as well as of shifts arising from other nuclear interactions. This effect is known as motional narrowing of

the NMR line, and is the reason why these lines are very sharp in molten ceramics, as opposed to several kHz broad in the solid.

In our experiments ^{27}Al free induction decay signals were typically acquired on our Varian 300 MHz solids spectrometer at settings of 50 kHz bandwidth, 40 W r.f. pulse power, 20 Hz pulse repetition frequency, 4096 point acquisition length and $175\ \mu\text{s}$ 90° r.f. pulse length. Very rapid ^{27}Al spin-lattice relaxation, due to substantial quadrupole coupling in ceramic melts, was observed in all molten samples.^{5,6} Temperature measurements were performed using the technique of spectroradiometry,^{6–8} and are accurate to $\pm 25^\circ\text{C}$. In the liquid state, the ^{27}Al chemical shift was found to be remarkably insensitive to temperature, varying less than 2 ppm from melting to 2450°C . This observation is generally consistent with previous measurements in molten alumina⁴ and in the $\text{CaO-Al}_2\text{O}_3$ system.⁹

Solid samples were characterized at room temperature by ^{27}Al and ^{31}P NMR measurements, performed either in the high temperature probe after sample melting and cooling, or separately in a type of probe used only for solids and called a Magic Angle Spinning (MAS) probe. In this probe, the sample is rapidly spun around an axis oriented at an angle θ , called the magic angle, with respect to H_0 . This angle is precisely set to satisfy the relation $3\cos^2\theta - 1 = 0$. The fast spinning, typically at frequencies from 3 to 10 kHz in our MAS probe, results in strong motional narrowing of NMR lines in solid samples and makes it possible to accurately determine their chemical shifts. For ^{31}P the standard reference used was 85 mol% H_3PO_4 in water, and MAS spectra were obtained at a spin rate of 6.5 kHz. ^{27}Al MAS spectra were also taken at room temperature, using as reference a solution of $\text{Al}(\text{NO}_3)_3$ at low concentration.

Raman spectra of quenched samples were obtained using a SpectraPhysics Model 2020 argon ion laser operating at 514.5 nm. Incident light is directed along the optical axis of an Olympus BH-2 microscope fitted with a Mitutoyo objective (SL50x with N.A. = 0.42). Backscattered radiation is collected and dispersed via a 600 groove/mm grating housed inside a Jobin Yvon Triax 550 spectrometer ($f = 0.55\ \text{m}$). The Raman signal is detected with a Princeton Instruments model 1100PB LN_2 -cooled CCD detector and Princeton Instruments Detector Controller. Spectra are processed and displayed on a desktop computer using CSMA Spectrometric Multichannel Analysis Software.

Electron microprobe measurements were performed on a JEOL JXA-8600 instrument in the Department of Chemistry and Biochemistry at Arizona State University. Electron probe samples were prepared by mounting shards of the quenched material in epoxy and polishing in a mineral oil medium. Water was avoided as a polishing medium since it was found that the presence of water could result in substantial alterations in the phosphate-containing samples. Powder and single crystal X-ray diffraction spectra were taken on a Siemens D5000 spectrometer in the department's X-ray Facility.

2.1. Synthesis of $(1-x)\text{Al}_2\text{O}_3:x\text{LaPO}_4$

Powders of the components were sintered, crushed, pressed, then melted in an image furnace and quenched in water, to form approximately spherical samples of diameter $\sim 3\ \text{mm}$. This sample morphology is required for levitation in the liquid-state NMR experiment. Starting values of LaPO_4 were 2, 5, 25, 50, 75, 87.5, and 100 mol%. X-ray diffraction and electron microprobe analysis of samples prepared by these procedures showed bulk compositions generally close to those of the starting materials, and in addition the presence of two or more phases. At least one of the phases was strongly alumina-rich, while another consisted mainly of LaPO_4 . MAS NMR of both ^{27}Al and ^{31}P in the solid state confirms this phase separation.

2.2. Synthesis of $(1-x)\text{C}_{12}\text{A}_7:x\text{LaPO}_4$ and $(1-x)\text{CA}:x\text{LaPO}_4$

These samples were made by a more complex procedure than the $\text{Al}_2\text{O}_3:x\text{LaPO}_4$ above. Starting materials for these sample preparations were AR grade $\text{Ca}(\text{OH})_2$ (J.T. Baker), and high purity Al_2O_3 (Mitutoyo Chemical Co., Tokyo), calcined 6 h at 600°C , then ball-mill mixed and melted to make C_{12}A_7 and CA. After synthesis of bulk C_{12}A_7 and CA, $\text{LaPO}_4 \cdot 5\text{H}_2\text{O}$ (Alza) was added in the amounts 12, 25, 50 and 75 mol% by ball-mill mixing, followed by sintering at $50\text{--}100^\circ\text{C}$ below the mixture's melting point (ranging from 1200 to 1600°C). This sequence of heating avoided loss of phosphate from the reaction mixture. The sintered ceramic was then re-powdered by ball mill, compressed into a rod mold at 5000 psi and resintered. The sintered rods were transformed into $\sim 3\ \text{mm}$ diameter glassy beads by rapid drop quenching into water in the image furnace.

3. Results: electron microprobe and X-ray

LaPO_4 dissolves or disperses into the ceramic melts, as evidenced by the disappearance of initially formed islands of monazite into the final drop-quenched beads. The beads themselves exhibit widely varying microstructures, some bearing microcrystalline structures while others appear strongly glass-like, depending on the initial compositions. In electron micrographs of most calcium-containing beads (CA-LaPO_4 and $\text{C}_{12}\text{A}_7\text{-LaPO}_4$ joins), only one phase is apparent. However, in some of these beads, phase separation was evident along both joins with distinct LaPO_4 regions (containing no Ca or Al) observed along grain boundaries between larger (Ca, La) aluminophosphate domains. The compositions of the different regions were determined from electron microprobe measurements. Electron microprobe analyses indicate that for samples prepared along the joins up to 50% LaPO_4 , the compositions within the large glassy regions were essentially the same as the nominal starting bulk compositions. However, in the C_{12}A_7 75% LaPO_4

sample, the glassy regions are somewhat depleted in LaPO_4 having an average LaPO_4 content of about 63% (± 3).

X-ray diffraction spectra were also taken on powdered samples of the drop-quenched beads. The diffraction patterns taken from the 75% LaPO_4 samples along both CA and C_{12}A_7 joins display very weak, sharp peaks of microcrystalline LaPO_4 , along with a much stronger, broad, amorphous background characteristic of a glass. The intensities of the small LaPO_4 peaks varies little from sample to sample.

The XRD line pattern in C_{12}A_7 :75% LaPO_4 also shows the presence of a double phosphate, $\text{LaCa}_3(\text{PO}_4)_3$.¹⁰ This compound apparently is only slightly soluble in the matrix of glassy alumina–calcia–monazite samples. As the LaPO_4 content is decreased along this join, the intensity of the diffraction peaks arising from the double phosphate is sharply reduced. In the 50% samples a careful analysis reveals only trace amounts in some samples, and in the 25% sample group we have been unable to detect its presence despite an extensive search.

4. NMR measurements: liquid samples

The chemical shift of ^{27}Al behaves differently for the three pseudo-binary melts studied, $(1-x)\text{Al}_2\text{O}_3:x\text{LaPO}_4$, $(1-x)\text{C}_{12}\text{A}_7:x\text{LaPO}_4$ and $(1-x)\text{CA}:x\text{LaPO}_4$. Fig. 2 shows our findings for $(1-x)\text{Al}_2\text{O}_3:x\text{LaPO}_4$ at temperatures near 2150 °C. The shift varies linearly with composition, starting at the 58.5 ppm value for pure alumina and increasing to 68 ppm at 75% LaPO_4 . Thus, the Al–O coordination in these samples becomes increasingly tetrahedral with LaPO_4 content. The LaPO_4 -rich limit of the Al chemical shift in these melts is approximately 72 ppm.

By contrast, for the C_{12}A_7 -based samples in the same temperature range the ^{27}Al shift does not depart from its strongly 4-coordinated value of 85 ppm, until the starting level of mon-

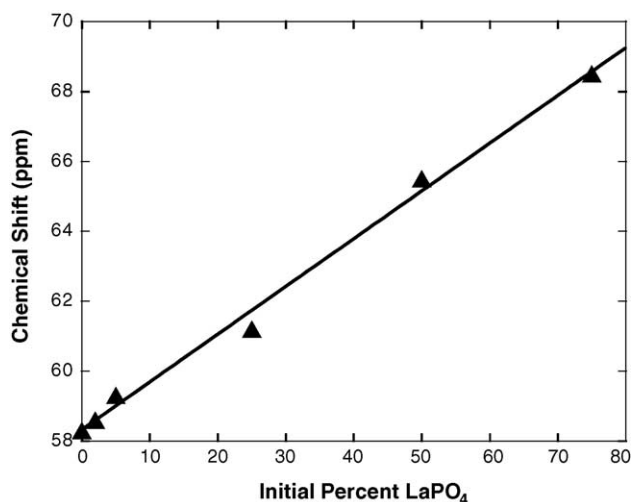


Fig. 2. Chemical shift of ^{27}Al vs. starting La-monazite mol% x , measured in $(1-x)\text{Al}_2\text{O}_3:x\text{LaPO}_4$ at temperatures near 2150 °C.

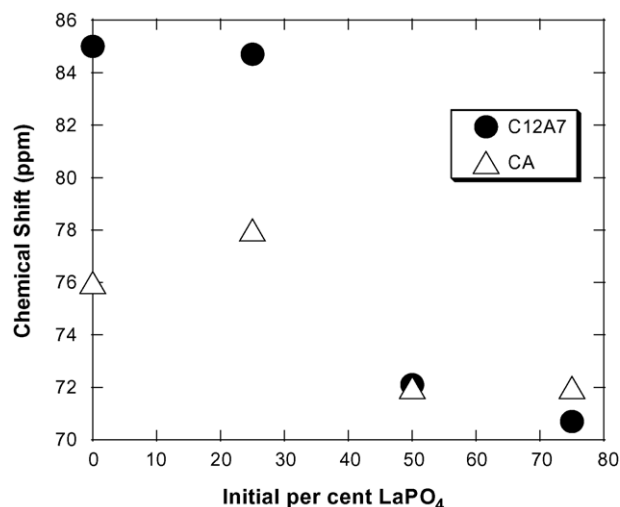


Fig. 3. Chemical shift of ^{27}Al vs. starting mol% LaPO_4 , measured in $(1-x)\text{C}_{12}\text{A}_7:x\text{LaPO}_4$ and in $(1-x)\text{CA}:x\text{LaPO}_4$ at temperatures near 2150 °C. Data for pure C_{12}A_7 and pure CA agree with those of Poe et al.¹¹

azite is between 25 and 50% (Fig. 3). Near this composition, the ^{27}Al chemical shift strongly decreases, approaching a value of ~ 71 ppm at high monazite fraction. Samples along the $(1-x)\text{CA}:x\text{LaPO}_4$ join show intermediate behavior, displaying a relatively weak dependence of Al chemical shift upon monazite content.

5. NMR measurements: quenched samples

Room temperature ^{27}Al chemical shifts of the samples show differences from as well as similarities to the liquid shifts of Figs. 2 and 3. Along the pure alumina–monazite join, there are no changes with composition, the shift remaining that of pure alumina over the entire range. This is consistent with EM and XRD observations of immiscibility of Al_2O_3 and LaPO_4 below melting along this join, providing further indication that the linear shift behavior of Fig. 2 is characteristic of atomic mixing of the two components in the melt.

Along the C_{12}A_7 – LaPO_4 join, however, strong variations of ^{27}Al shift with composition occur, as seen in Fig. 4. The glass shifts lie below those of the solid, but remain in the range of tetrahedral Al–O coordination until 50% LaPO_4 , where the ^{27}Al NMR line's width strongly increases and its peak position dramatically decreases to ~ 10 ppm, within the range of five-fold coordination in phosphate glasses. Al has thus become largely five-fold coordinated in the 50% LaPO_4 glass, whereas it remains mainly tetrahedrally coordinated in the liquid, in Fig. 3. This change is taken to mean that the glass transition quenches in a melt structure characteristic of a temperature well below those of our levitated melts, where our NMR data were taken. Such a temperature is known as the fictive temperature of the glass, and is dependent upon several factors, notably the rate of cooling of the sample.

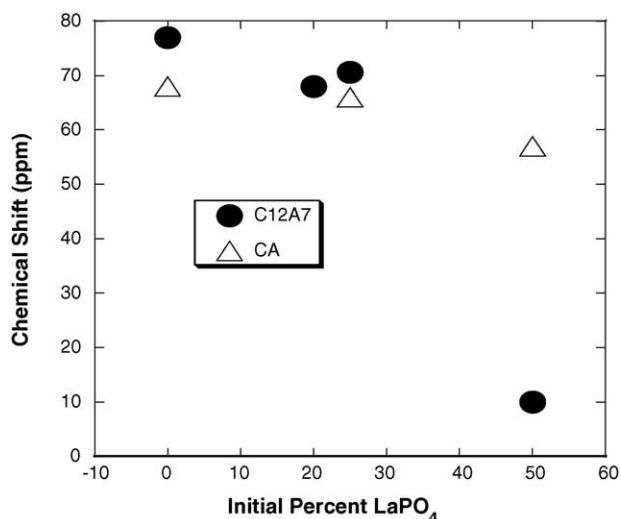


Fig. 4. Chemical shift of ^{27}Al vs. starting mol% LaPO_4 for CA and C_{12}A_7 -based glassy samples, at room temperature.

Strong changes of melt structure with temperature can be indicators of the onset of polyamorphic behavior.

In liquid samples the NMR line of ^{31}P has yet to be observed, whereas it is easily seen in the reference 85 mol% H_3PO_4 solution and in the magic angle spinning (MAS) spectra of water-quenched samples containing La-monazite. We are investigating possible reasons for our inability to detect signals from ^{31}P in melts, but our current view is that phosphorus sites are widely distributed in the liquid, which results in a very broad NMR line. In quenched samples a strong ^{31}P signal is observed, which typically yields a spectrum like that of C_{12}A_7 :25% LaPO_4 , shown in Fig. 5.

Our observed ^{31}P NMR spectra can be interpreted in terms of the local bonding arrangement or “speciation” of the phos-

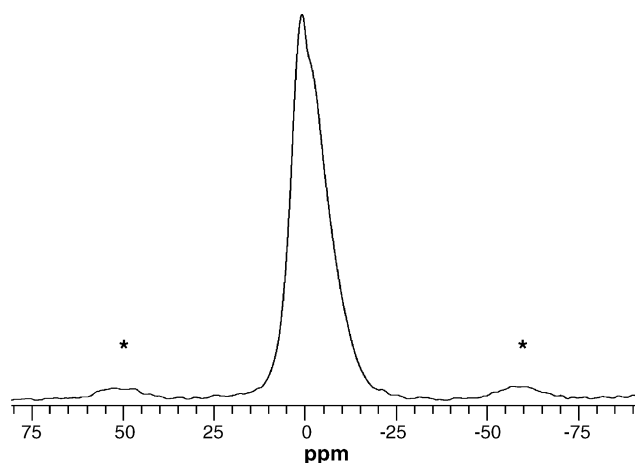


Fig. 5. ^{31}P MAS NMR spectrum of quenched C_{12}A_7 :25% LaPO_4 at room temperature. The two peaks with asterisks (*) are sidebands, due to modulation of NMR frequencies by the sample spinning at 6.5 kHz. (NMR spectra are plotted with chemical shift increasing to the left, for physical and chemical reasons not discussed here.)

phorous in the glass. In phosphate glasses, this bonding structure is often described in terms of the degree of polymerization of the individual tetrahedral PO_4 groups; this speciation distribution is expressed in terms of a Q^n label. Here, n refers to the number of oxygen atoms on a given phosphorus tetrahedron that are corner-linked (or “bridged”) to other phosphorus tetrahedral units. (It is important to clarify that in some literature the n refers to the number of oxygen atoms bridged to any tetrahedrally coordinated metal.) In the compositional joins investigated in this study, the oxygen to phosphorous ratio exceeds 4, and hence it is expected that most of the phosphorous would exist as completely depolymerized Q^0 species.

The ^{31}P NMR spectrum for the quenched glasses of our samples is generally characterized by a strong broad band near 0 ppm. There appear to be two components in this band: a relatively sharp feature at +2 ppm and a substantial shoulder at about -4 ppm. Similar ^{31}P spectra are found for other LaPO_4 concentrations, with the exception of 75%, where an additional weak shoulder appears at more negative chemical shift values.

In alumina-free alkali and alkaline earth phosphate glasses, the phosphorous chemical shift for Q^0 units occurs near -13 ppm and near 0 ppm for Q^1 units.^{12,13} These assignments, however, may not be appropriate for the alumina phosphate glasses studied here. It has been previously established that Al in the second coordination sphere of phosphorous significantly increases the shielding (more negative chemical shift) of the P nucleus. At compositions of our glasses, we expect one or more Al atoms in the second coordination sphere of P (i.e., P-O-Al linkages). Such linkages give rise to a decrease in ^{31}P shift values (in comparison with those of alkali and alkaline earth phosphates), of magnitude approximately 6 ppm per linkage (see Dollase et al.¹⁴ and recently Schneider et al.¹⁵). The decreases are observed whether P is linked to Al tetrahedral units (Dollase et al.) or Al octahedral units (Schneider et al.). Thus, our ^{31}P shifts could also arise from Q^0 units (no P-O-P linkages), but with linkages to nearby Al cations. This interpretation is also consistent with the Raman data presented below, in which a sharp 960 cm^{-1} feature in the Raman spectrum is attributed to orthophosphate Q^0 groups.

6. Raman spectra

The Raman spectrum of a melted and water-quenched sample of C_{12}A_7 containing 50% LaPO_4 is shown in Fig. 6. The spectrum displays broad features, indicative of a glassy material. No evidence for large crystalline regions was found under the $3\text{ }\mu\text{m}$ spatial resolution of the Raman microprobe, consistent with the electron microprobe and X-ray diffraction measurements.

Complementary to NMR, Raman spectroscopy is also a sensitive probe for elucidating the local and intermediate range order in phosphate and aluminophosphate glasses. The

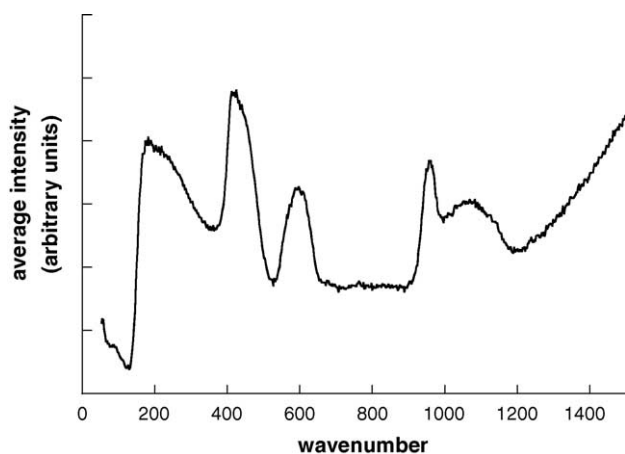


Fig. 6. Raman spectrum of glassy $C_{12}A_7:50\%$ $LaPO_4$.

spectral region between 900 and 1200 cm^{-1} is typically associated with the stretching vibrations of the PO_4 units in these systems. The sharp peak near 960 cm^{-1} , observed in the spectra for all of our samples containing between 25 and 75% $LaPO_4$, is the diagnostic feature for non-bridging Q^0 orthophosphate groups and arises from the strongly Raman active symmetric stretching vibration of this unit.

A broad band centered near 1100 cm^{-1} is also observed in this high frequency region. The assignment of this band is less definitive. It occurs in the spectral region associated with both corner-linked Q^1 and Q^2 phosphate groups (pyrophosphate units and metaphosphate chains, respectively).^{15,16} However, PO_4 units corner linked to other phosphorus tetrahedra (i.e., Q^1 , Q^2 and Q^3 species) would also display a symmetric P–O–P vibration near $700\text{--}750\text{ cm}^{-1}$. The absence of this band in our spectra indicates that all of the phosphorous tetrahedral are isolated or depolymerized from other phosphorous units.

The 1100 cm^{-1} region has also been assigned to phosphate stretching deformations in $AlPO_7$ units, where a Q^0 phosphorous tetrahedron is corner linked to AlO_4 . This interpretation is consistent with the Raman scattering observed in the lower frequency region for our samples. There is also evidence from the Raman spectrum of crystalline $AlPO_4$ that Al acts to shift the orthophosphate Raman lines to higher wavenumbers.¹⁷ In the low cristobalite form of $AlPO_4$, Al and P are both tetrahedrally coordinated and alternately linked through corner-sharing tetrahedra. In this compound, all of the P atoms are Q^0 species and the PO_4 stretching vibration occurs near 1100 cm^{-1} . It is plausible that the spectral intensity in the region near 1100 cm^{-1} in the 50% $LaPO_4$ sample could arise from PO_4 tetrahedra that are strongly associated with Al, perhaps $AlPO_7$ structural units. Its breadth may also be due to the presence of a distribution of species involving Al with the other charge-balancing cations (La and Ca).

The strong band observed near 600 cm^{-1} is consistent with symmetric Al–O–Al stretching vibrations of corner-linked aluminate tetrahedra.

7. Discussion

Based upon the ^{27}Al chemical shift results, the effects of $LaPO_4$ upon Al bonding in the three groups of molten samples appear to differ significantly. Along the Al_2O_3 – $LaPO_4$ join, the linear increase of shift with increasing $LaPO_4$ reflects a gradually increasing tetrahedral coordination of Al in the liquid.¹⁸ Molten Al_2O_3 is believed to contain a mixture of four-, five- and six-coordinate Al species at these temperatures.¹⁹ Furthermore, there is no indication of $LaPO_4$ saturation in the melt along the Al_2O_3 – $LaPO_4$ join. The Al chemical shift of the melt increases continually over the entire composition range.

In $(1-x)CA:xLaPO_4$ melts there are small but definite variations in chemical shift with monazite concentration. The Al chemical shift for pure CA is close to that in highly $LaPO_4$ -rich samples, in part because of tetrahedral Al ion's relative insensitivity to second neighbor atoms, which change from Al and Ca to P and La as $LaPO_4$ fractions increase. In $C_{12}A_7$ melts Al resides essentially entirely in tetrahedral sites (the ^{27}Al shift is 85 ppm in the melt). Addition of $LaPO_4$ to the melt has little effect upon this coordination to values as high as 25%, but by 50% there is a significant decrease in chemical shift to ~ 72 ppm. This change is more pronounced in the quenched glasses along this same join, which suggests a substantial dependence of the melt structure upon temperature in this compositional regime. In particular, at 50% $LaPO_4$ the ^{27}Al chemical shift drops to as low as 10 ppm, indicating a substantial fraction of high coordinate (5- and 6-coordinate) aluminum at the glass transition temperature. We are presently undertaking investigations of the underlying factors responsible for these dramatic changes of melt structure. We note that in contrast to phosphorus, aluminum is considered to be capable in phosphate glasses of acting both as a network former and a network modifier.¹⁵ As a modifier, Al has been shown to cross-link PO_4 tetrahedra, in which circumstance it would compete with other modifiers such as NaO and CaO. This situation appears to occur in our CaO-containing samples.

Another feature of interest is that at the highest monazite starting concentration studied (75%) formation of the recently studied double phosphate $LaCa_3(PO_4)_3$ is observed in quenched samples.¹⁰ Since this compound melts congruently at 1890°C , and our samples are quenched from temperatures well above this value, the double phosphate's precipitation most likely occurs during quench. Electron microprobe measurements in the 25% sample, showing a lack of Ca in the small $LaPO_4$ crystalline grains along with the absence of any X-ray pattern from the double phosphate $LaCa_3(PO_4)_3$, indicate that for this $LaPO_4$ fraction the double phosphate, if present, is atomically mixed with $C_{12}A_7$. Nonetheless, the coordination of Al remains strongly four-fold in the melt. In the 50% sample, the upper limits on La fraction for such mixing are evidently exceeded, although only slightly. At 75%, precipitation of the double phosphate is clearly apparent, though still not extensive. The strong decrease in observed

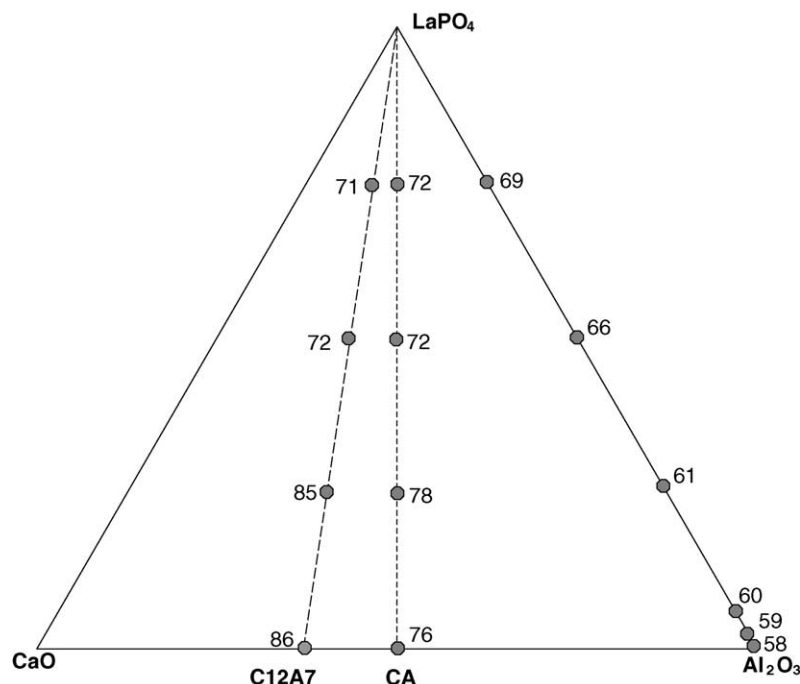


Fig. 7. Chemical shifts of ^{27}Al and compositions in the $\text{CaO}-\text{Al}_2\text{O}_3-\text{LaPO}_4$ system. More data along the $\text{CaO}-\text{Al}_2\text{O}_3$ join can be found in Poe et al.^{11,20}

liquid-state ^{27}Al chemical shift noted above, from 25% to 50 and 75% samples, may be related to the onset of this precipitation.

Fig. 7 shows a composition diagram annotated with ^{27}Al chemical shifts along all three joins, based on the values shown in Figs. 2 and 3 for the $\text{CaO}-\text{Al}_2\text{O}_3$ join. We conclude that the shift for LaPO_4 melts having low Al impurity content should be approximately 70 ppm, regardless of other, non-Al containing impurities.

Acknowledgements

This work was co-funded by the National Science Foundation and the Air Force Office of Scientific Research, under NSF grant DRM01-116361. It is also based on work supported by the National Science Foundation under Grant No. DMR 9818133. Further support for ultra high temperature NMR studies has been provided by the Research Corporation, under grant RA-0276. We wish to thank R. Weber of Containerless Corp. for many helpful discussions.

References

- Massiot, D., Taulelle, F. and Coutures, J.-P., Structural diagnostic of high temperature liquid phases by ^{27}Al NMR. *Colloq. Phys.*, 1990, **51C5**(Suppl. 18), 425.
- Coutures, J.-P., Massiot, D., Bessada, C., Echegut, P., Rifflet, J.-C. and Taulelle, F., Etude par RMN ^{27}Al d'aluminates liquides dans le domaine 1600–2100 °C. *C. R. Acad. Sci. Paris*, 1990, **310**, 1041.
- Taulelle, F., Coutures, J.-P., Massiot, D. and Rifflet, J.-C., High and very high temperature NMR. *Bull. Magn. Reson.*, 1990, **11**, 314.
- Florian, P., Massiot, D., Poe, B., Farnan, I. and Coutures, J.-P., A time resolved ^{27}Al NMR study of the cooling process of liquid alumina from 2450 °C to crystallization. *Solid State Nuclear Magn. Reson.*, 1995, **5**, 233–238.
- Marzke, R. F., Piwowarczyk, J., McMillan, P.F. and Wolf, G.H., Al motion rates in levitated, molten Al_2O_3 samples, measured by Pulsed Gradient Spin Echo ^{27}Al NMR. Accompanying paper in this volume.
- Piwowarczyk, J., *Aluminum-27 Nuclear Magnetic Resonance Study of Molten Aluminum-bearing Oxides*. M.S. Thesis, Arizona State University, May 2001.
- For description of this technique applied to temperature measurements in the diamond anvil cell, see Heinz, D. and Jeanloz, R., Temperature measurements in the laser-heated diamond cell. In *High Pressure Research in Mineral Physics*, ed. M. H. Manghnani and Y. Syono. Terra Scientific, Tokyo, 1987, pp. 113–1274.
- Jephcoat, A. P. and Besedin, S. P., Temperature measurement and melting determination in the laser-heated diamond-anvil cell. *Phil. Trans. R. Soc. Lond. A*, 1996, **354**, 1333–1360.
- Touzo, B., Trumeau, D., Massiot, D., Farnan, I. and Coutures, J.-P., High temperature ^{27}Al NMR time resolved study. Application to the $\text{CaO}-\text{Al}_2\text{O}_3$ binary system. *J. Chim. Phys.*, 1995, **92**, 1871–1876.
- Jungowska, W., The system $\text{LaPO}_4-\text{Ca}_3(\text{PO}_4)_2$. *Solid State Sci.*, 2002, **4**, 229–232.
- Poe, B. T., McMillan, P. F., Coté, B., Massiot, D. and Coutures, J.-P., Structure and dynamics in calcium aluminate liquids: high-temperature ^{27}Al NMR and Raman spectroscopy. *J. Am. Ceram. Soc.*, 1994, **77**, 1832–1888.
- Brow, R. K., Review: the structure of simple phosphate glasses. *J. Non-Cryst. Solids*, 2000, **263–264**, 1–28.
- Hartmann, P. T., Vogel, J., Friedrich, U. and Jager, C., Nuclear magnetic resonance investigations of aluminum containing phosphate glass-ceramics. *J. Non-Cryst. Solids*, 2000, **263–264**, 94–100.
- Dollase, W. A., Merwin, L. H. and Sebal, A., Structure of $\text{Na}_{3-3x}\text{Al}_x\text{PO}_4$, $x=0$ to 0.5. *J. Solid State Chem.*, 1989, **83**, 140–149.

15. Schneider, J., Oliveira, S. L., Nunes, L. A. O. and Panepucci, H., Local structure of sodium aluminate metaphosphate glasses. *J. Am. Ceram. Soc.*, 2003, **86**, 317–324.
16. Exarhos, G., Vibrational studies of glass structure and localized interactions. In *Structure and Bonding in Non-Crystalline Solids*, ed. G. Walrafen and A. Revesz. Plenum Press, 1986, pp. 203–217.
17. Gregora, I., Magneron, N., Simon, P., Luspín, Y., Raimboux, N. and Phillopot, E., Raman study of AlPO_4 (berlinite) at the α - β transition. *J. Phys.: Condens. Matter*, 2003, **15**, 4487–4501.
18. Yarger, J. L., Smith, K. H., Nieman, R. A., Diefenbacher, J., Wolf, G. H., Poe, B. T. et al., Al coordination changes in high-pressure aluminosilicate liquids. *Science*, 1996, **270**, 1964–2019.
19. Landron, C., Hennem, L., Jenkins, T. E., Greaves, G. N., Coutures, J. P. and Soper, A. K., Liquid alumina: detailed atomic coordination determined from neutron diffraction data using empirical potential structure refinement. *Phys. Rev. Lett.*, 2001, **86**, 4839–4842.
20. Poe, B. T., McMillan, P. F., Coté, B., Massiot, D. and Coutures, J.-P., Magnesium and calcium aluminate liquids: in situ high-temperature ^{27}Al NMR spectroscopy. *Science*, 1993, **259**, 786–788.